

COMMUNICATION

View Article Online
View Journal | View IssueCite this: *Org. Biomol. Chem.*, 2021, **19**, 8025Received 30th July 2021,
Accepted 27th August 2021

DOI: 10.1039/d1ob01343b

rsc.li/obc

Efficient synthesis of isoindolones by intramolecular cyclisation of pyridinylbenzoic acids†

Atena B. Solea,^{a,b} Sining Wang,^c Xiao-Song Xue,^c Aurelien Crochet,^b Katharina M. Fromm,^b Kendall N. Houk,^c Olimpia Mamula^{*a} and Christophe Allemann^{†a}

A straightforward one-pot method for the synthesis of unreported pyrido-[2,1-*a*]isoindolones in excellent yield is described. Two novel isoindolones were synthesized and fully characterized. The alkyl substituents on the pyridine play an important role in the outcome of the reaction. The mechanism, investigated through DFT calculations, features an unprecedented intramolecular cyclization reaction involving a carboxylic acid activated by tosyl chloride and an electron-poor pyridinic nitrogen. This protocol completes the known strategies to obtain functionalized isoindolones.

The isoindolone structure is an important structural motif found in various natural products or compounds of pharmaceutical interest.¹ In particular, derivatives of pyrido-[2,1-*a*]isoindolones are present in natural alkaloids such as (±)-nuevamine, or biologically-active compounds such as valmerin² or urotesin-II receptor antagonists³ (Fig. 1). When the isoindolone structure is polyconjugated, interesting emissive properties are obtained, making such compounds promising organic dyes for bioimaging applications.^{4,5} Such a case is batracylin⁶ which is an antitumor agent and also contains the structural motif of various emissive materials due to its polyconjugated structure.⁷

Several methods for the synthesis of functionalized isoindolones have been reported, but the yields are rather low to moderate. For example, the typical reaction pathways for isoindolone synthesis are based on Diels-Alder or anionic cyclizations,^{8,9} intramolecular cyclization¹⁰ the Heck reac-

tion,¹¹ Mannich-type reaction,¹² radical cyclization of enamine or ynamide derivatives^{13,14} sulfa-Michael-triggered tandem reaction¹⁵ or olefin methathesis.¹⁶ Besides these intermolecular methods, two examples of intramolecular attack from a pyridinic N atom towards either a biacetate,¹⁷ or an aldehyde^{5,18–21} have been reported. These are rare cases of *N*-acyliminium ion formation from an electron-poor heterocycle like pyridine,²² so any such observation is of major interest from a synthetic point of view.

We are reporting here this type of intramolecular cyclization in which the pyridinic nitrogen atom is performing a nucleophilic attack towards the tosylated carboxylic acid derivative, followed by deprotonation of the annealed ring. The novelty of

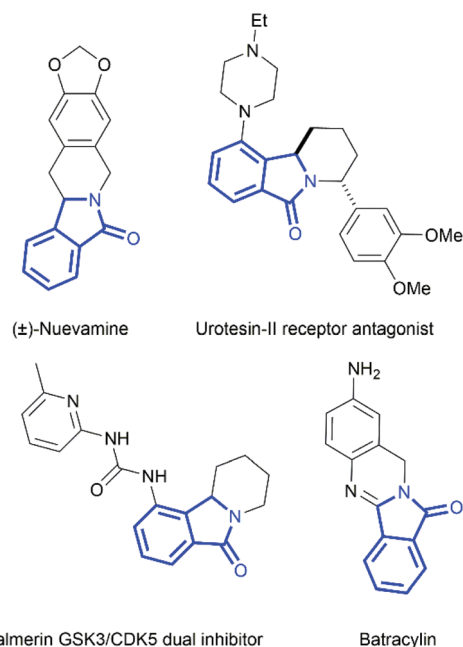


Fig. 1 Selected examples of bioactive molecules with an isoindolone core.

^aUniversity of Applied Sciences of Western Switzerland, HES-SO, HEIA-FR, PÉrolles 80, CH-1705 Fribourg, Switzerland. E-mail: olimpia.mamulasteiner@hefr.ch, christophe.allemann@hefr.ch

^bUniversity of Fribourg, Department of Chemistry, Chemin du Musée 9, CH-1700 Fribourg, Switzerland

^cDepartment of Chemistry and Biochemistry, University of California, Los Angeles, California 90095, USA

†Electronic supplementary information (ESI) available: Experimental section, photophysical characterisation, copies of NMR spectra, computational details, X-ray tables. CCDC 2036677–2036679. For ESI and crystallographic data in CIF or other electronic format see DOI: 10.1039/d1ob01343b

our work lies in the participation of a carboxylic acid instead of the aldehyde that Mamane and coworkers used in their work.¹⁸ Moreover, the *N*-acylamonium intermediate does not undergo rearrangement but it is stabilized by the deprotonation of the carbon at the β position of the nitrogen atom. Indeed, the typical conditions leading to anhydride formation (TsCl in basic media) did not give the expected product (SA, see Scheme 1), but a chiral isoindolone *via* an unprecedented cyclization reaction. Two novel isoindolones were fully characterized in solution and solid state and a mechanism based on DFT calculations is proposed.

The brominated precursor **1** was obtained through a reported procedure²³ and subsequently underwent lithiation and carboxylation with gaseous CO₂ to give the chiral pinene-pyridine carboxylic acid **2** (Scheme 1). The formation of **2** was confirmed in solution by NMR and HRMS and in the solid state by single crystal X-ray diffraction (Fig. 2). Compound **2** crystallizes in the *P*₂₁₂₁₂ (no. 18) space group with two molecules in the asymmetric unit. The two molecules interact through middle strength intermolecular H-bonding between the N of the pyridine atom and the carboxylic acid group (Fig. S1†). Deprotonation and tosylation of **2**, following a modified version of a reported procedure,²⁴ did not give the expected anhydride. Instead, the orange compound **3** was isolated in excellent yield.

The structure of **3** was confirmed by single crystal X-ray diffraction as shown in Fig. 2. The compound crystallizes with one molecule in the asymmetric unit in the *P*₂₁₂₁₂ (no. 19)

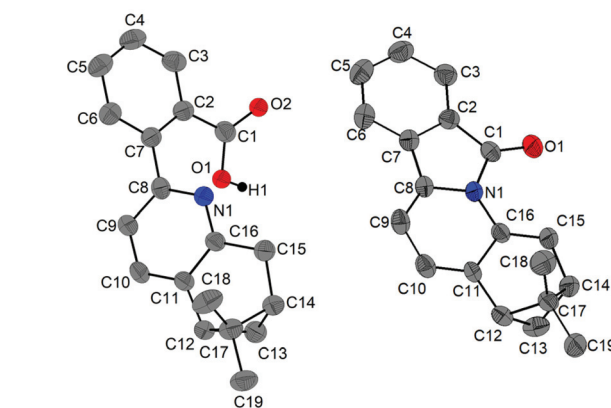
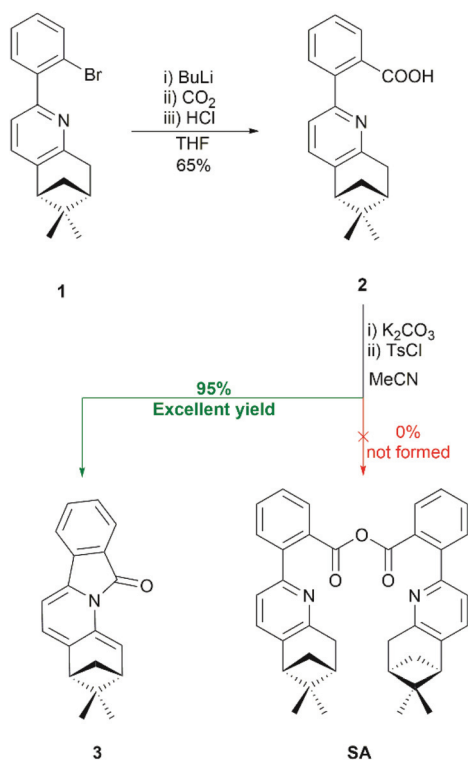


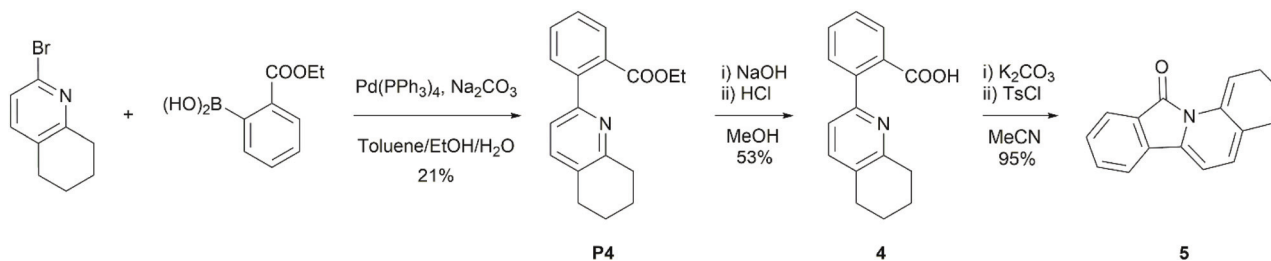
Fig. 2 Molecular structure of **2** (left) and **3** (right) determined by single-crystal X-ray diffraction with ellipsoids at 30% probability with atom numbering scheme. The H atoms were omitted for clarity.

space group. The bond lengths C8–C9, C10–C11 and C15–C16 are in the expected range for double bonds (1.340(5), 1.338(5) and 1.331(5) Å, respectively), whereas the bond length C9–C10 is between a single and a double bond (1.439(5) Å). In comparison, the bond lengths C8–C9, C9–C10 and C10–C11 in compound **2** are typical for aromatic, conjugated structures (1.382(8), 1.391(8), 1.380(8) Å, respectively), while the C15–C16 bond from the pinene unit is clearly a single bond, with a length of 1.496(7) Å. More precisely, for compound **3**, the bond orders for C8–C9 and C10–C11 are indicative of a double bond (1.7093 and 1.7716, respectively), whereas the bond C9–C10 indicates that this bond has more of a single bond character (1.0913), suggesting decreased delocalization in the pyridine ring of the precursor **2** (Fig. S2; details for bond order calculation are provided in the ESI†). Each molecule is interacting with a neighbouring one through strong face-to-face π – π stacking interactions between the phenyl and the lactam rings, with centroid–centroid distances of 3.6 Å (Fig. S3†). The structure of **3** was further confirmed in the solid state through IR, where a strong band at 1660 cm^{−1} was observed, corresponding to the C=O stretch typical for an isoindolonic structure (Fig. S4†). In solution, an interesting feature of the ¹H-NMR spectrum of **3** is the downfield shift of the vinyl proton H15 at 7.41 ppm, in contrast to the doublet at 3.23 ppm observed for the protons in β position to the pyridinic N-atom in the starting material **2** (Fig. S5†). The formation of the isoindolone ring is also visible on the UV-Vis and emission spectra. Whereas compound **2** does not absorb in the visible region nor have any visible emission, compound **3** shows a strong absorption band with a maximum at 474 nm (Fig. S6†). Moreover, when excited at this wavelength, compound **3** emits in the visible region, with a λ_{em} = 588 nm (Fig. S7†).

The same reaction conditions used to obtain **3** were applied to the achiral, cyclohexyl-pyridine analogue **4**, which was obtained through a Suzuki coupling (Scheme 2), followed by hydrolysis of the ethyl ester **P4**. This reaction gave the isoindolone **5** in excellent yield. The pyrido-[2,1-*a*]isoindolonic struc-



Scheme 1 Synthetic steps for obtaining **3**.



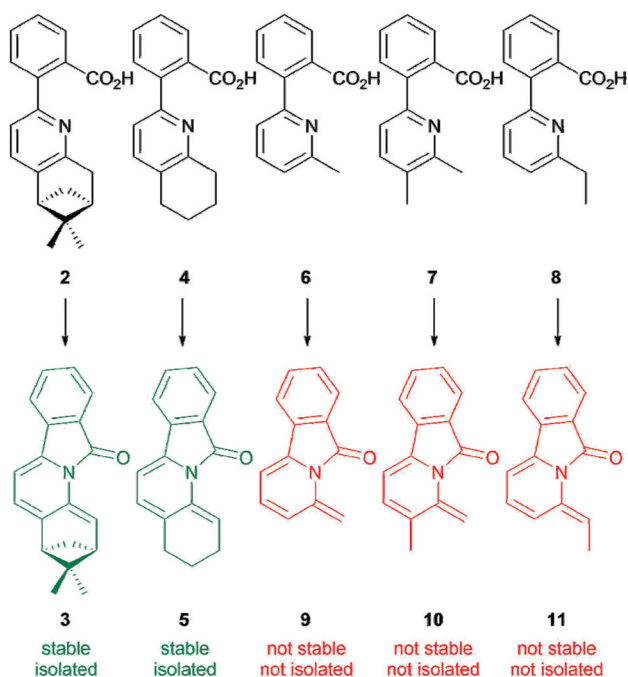
Scheme 2 Synthesis of the achiral analogue 5.

ture of 5 was confirmed in solution by NMR, UV-Vis and emission spectroscopy, HRMS and by IR in solid state. As in the case of compound 3, the ^1H -NMR spectrum of 5 shows a strong downfield shift for the proton in β -position with respect to the N atom at 7.40 ppm, as well as shifts around 6–6.5 ppm for the vinylic atoms from the former pyridine ring (Fig. S8†). The photophysical properties of 5 are similar to the ones of 3, with a similar UV-Vis spectrum and a broad absorption band with a maximum at $\lambda_{\text{abs}} = 472$ nm (Fig. S9†) and a maximum of emission at $\lambda_{\text{em}} = 567$ nm (Fig. S10†). The IR spectrum of 5 is also very similar to the IR spectrum of 3, with a strong band at 1681 cm^{-1} (Fig. S4†), stemming from the C=O stretching from the isoindolone moiety. The sterically less hindered, but also more electron-deficient, *ortho*-methyl, dimethyl, and ethyl derivatives 6, 7, 8 (Scheme 3) were also used as substrates. The corresponding isoindolones 9, 10, and 11 could not be isolated. As the substrates 6, 7, and 8 were not soluble in acetonitrile, the reaction was done in acetone. NMR titration experi-

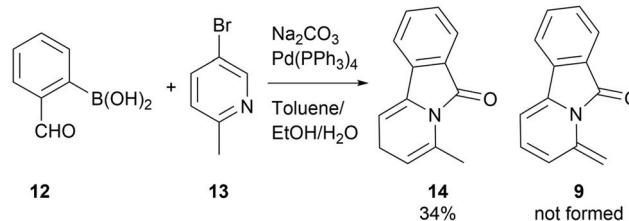
ments showed signals corresponding to isoindolones (9–11, Fig. S11–S16†). Moreover, ESI-MS spectra (Fig. S17 and S18†) of the reaction mixture showed molecular peaks of the isoindolones. Thus, the scope of this reaction is limited to cyclic substituent on the pyridinic moiety. Substrates with aliphatic substituents like ethyl or methyl at the *ortho* position form the isoindolone ring but the resulting products are unstable and degrade before isolation. Moreover, in the original solvent (acetonitrile), these substrates are not soluble and mass transfer is most probably limiting the reaction.

In order to check the stability of 9 and to investigate a possible deprotonation of the *ortho* methyl unit, we performed a previously reported reaction which also involves a nucleophilic attack from a pyridinic nitrogen towards an aldehyde group.¹⁸ Instead of starting from the carboxylic acid derivative of a bipyridine, we have made a Suzuki cross-coupling of 2-formylphenylboronic acid 12 and 2-bromo-6-methylpyridine 13 under the reactions conditions described by Mamane and co-workers.¹⁸ As shown in Scheme 4, the desired isoindolone 9 was not obtained. Instead of the triene 9, a stable diene 14 has been easily isolated and purified by column chromatography. We can conclude, that the reaction discussed in this paper is significantly different compared with the one described by Mamane and Igeta. Moreover, the oxidation of the pyridino isoindolones with Ag_2O ²⁵ reported by Mamane and co-workers leads to the formation of an ester moiety, indicating thus a difference in oxidation states between our product and theirs.

Based on the experimental data, we propose the following three-part mechanism: (A) the carboxylic acid is first activated by TsCl; (B) the activated acid then undergoes intramolecular cyclization through an *N*-nucleophilic attack; (C) the resulting intermediate is deprotonated either by the resulting ^-OTs



Scheme 3 Substrates and products that have been investigated. Reaction conditions: K_2CO_3 , TsCl in acetonitrile (for products in green), or Et_3N , TsCl in acetone- d_6 (for products in red).



Scheme 4 Synthesis of the methylated derivatives under Mamane and Igeta's reaction conditions.¹⁸

from (B) or HCO_3^- . To evaluate the plausibility of our proposed mechanism, we performed density functional theory (DFT) calculations (Fig. 3). Our computational studies indicated a substantially exergonic pathway. The intramolecular cyclization step (TS1) is a facile step due to the leaving group ability of $^- \text{OTs}$, with an activation barrier of $7.3 \text{ kcal mol}^{-1}$. Following cyclization, the deprotonation by HCO_3^- (TS2b; overall $\Delta G^\ddagger = 10.0 \text{ kcal mol}^{-1}$) proceeds with a more favorable activation barrier compared to that by $^- \text{OTs}$ (TS2a; $\Delta G^\ddagger = 19.1 \text{ kcal mol}^{-1}$). The release of H_2CO_3 is mildly endergonic by our calculations, although this process is expected to be entropically

favorable. This can be explained by the breakage of a strong hydrogen bond between the product and H_2CO_3 (complex-2b), which is enthalpically unfavorable. Overall, our calculations indicate that an intramolecular cyclization followed by HCO_3^- deprotonation leads to a free energy change of $-34.9 \text{ kcal mol}^{-1}$, in line with our hypothesis. The energy of the expected anhydride product was also calculated, and to our surprise, the anhydride was very stable ($\Delta G = -47.4 \text{ kcal mol}^{-1}$, relative to the reactant). The anhydride was not detected in the reaction mixture, thus its formation is presumed to be kinetically unfavorable due to its bimolecular nature. Details of compu-

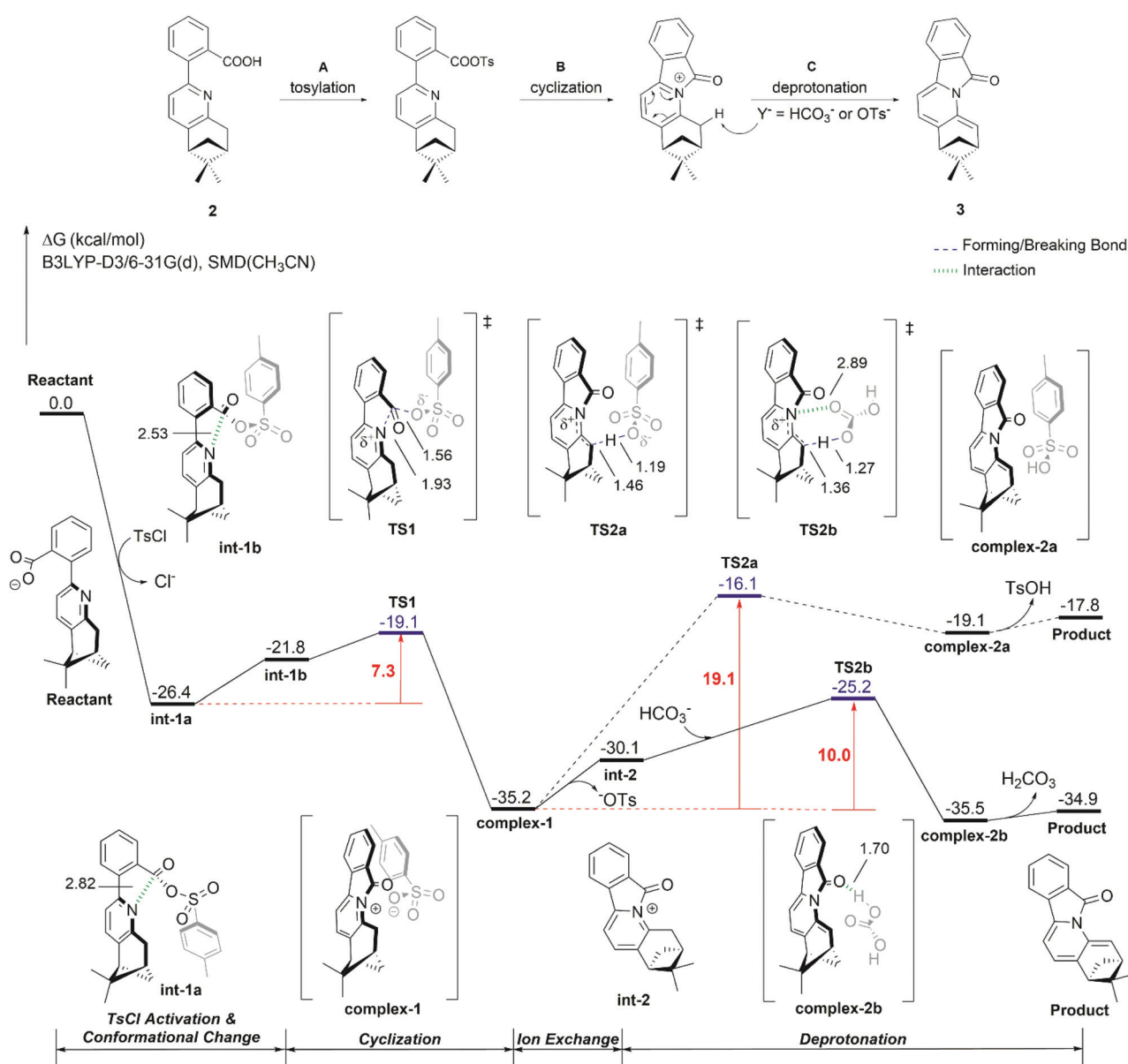


Fig. 3 Overview of the pinene-pyrido[2,1,a]isoindolone **3** formation (top) and free energy profile (in kcal mol^{-1}) for the proposed mechanism calculated at the B3LYP-D3/6-31G(d), SMD(CH_3CN) level of theory (bottom). All intermediate structures were obtained from IRC, with the exception of int-1a and int-2 (conformational search, see ESI†). Ion exchange pertains to the displacement of $^- \text{OTs}$ by HCO_3^- . Interatomic distances are marked in Ångstroms.

tational methodologies used in this study are provided in the ESI.†

Conclusions

In conclusion, a new synthetic pathway for obtaining unsaturated pyrido-[2,1-*a*]isoindolones from electron-poor heterocycles was developed. With our procedure, we successfully synthesized chiral and achiral isoindolone derivatives annelated to deprotonated pinene (3) and cyclohexyl (5) rings in excellent yield. Through DFT calculations, the mechanism of the reaction was elucidated.

Conflicts of interest

There are no conflicts to declare.

Acknowledgements

The authors wish to thank Dr Albert Ruggi (University of Fribourg) for measuring the Mass Spectra and Sandrine Aeby (HEIA-FR) for assisting with the precursor synthesis.

Notes and references

- 1 K. Speck and T. Magauer, *Beilstein J. Org. Chem.*, 2013, **9**, 2048–2078.
- 2 X. Li, X. Wang, Z. Tian, H. Zhao, D. Liang, W. Li, Y. Qiu and S. Lu, *J. Mol. Model.*, 2014, **20**, 2407.
- 3 D. K. Luci, E. C. Lawson, S. Ghosh, W. A. Kinney, C. E. Smith, J. Qi, Y. Wang, L. K. Minor and B. E. Maryanoff, *Tetrahedron Lett.*, 2009, **50**, 4958–4961.
- 4 Y. A. Amador-Sánchez, A. Aguilar-Granda, R. Flores-Cruz, D. González-Calderón, C. Orta, B. Rodríguez-Molina, A. Jiménez-Sánchez and L. D. Miranda, *J. Org. Chem.*, 2020, **85**, 633–649.
- 5 Z. El Abidine Chamas, E. Marchi, A. Modelli, Y. Fort, P. Ceroni and V. Mamane, *Eur. J. Org. Chem.*, 2013, 2316–2324.
- 6 V. A. Rao, K. Agama, S. Holbeck and Y. Pommier, *Cancer Res.*, 2007, **67**, 9971–9979.
- 7 U. Warde, L. Rhyman, P. Ramasami and N. Sekar, *J. Fluoresc.*, 2015, **25**, 685–694.
- 8 M. Ball, A. Boyd, G. Churchill, M. Cuthbert, M. Drew, M. Fielding, G. Ford, L. Frodsham, M. Golden, K. Leslie, S. Lyons, B. McKeever-Abbas, A. Stark, P. Tomlin, S. Gottschling, A. Hajar, J. L. Jiang, J. Lo and B. Suchozak, *Org. Process Res. Dev.*, 2012, **16**, 741–747.
- 9 D. L. Comins and Y. M. Zhang, *J. Am. Chem. Soc.*, 1996, **118**, 12248–12249.
- 10 S. Wang, L. Cao, H. Shi, Y. Dong, J. Sun and Y. Hu, *Chem. Pharm. Bull.*, 2005, **53**, 67–71.
- 11 D. L. Comins, S. P. Joseph and Y. M. Zhang, *Tetrahedron Lett.*, 1996, **37**, 793–796.
- 12 A. Alsarabi, J. L. Canet and Y. Troin, *Tetrahedron Lett.*, 2004, **45**, 9003–9006.
- 13 S. Gowrisankar, S. J. Kim, J. E. Lee and J. N. Kim, *Tetrahedron Lett.*, 2007, **48**, 4419–4422.
- 14 F. Marion, C. Courillon and M. Malacria, *Org. Lett.*, 2003, **5**, 5095–5097.
- 15 T. Y. Qin, L. Cheng, J. Ho-Chol, S. X. A. Zhang and W. W. Liao, *Synthesis*, 2016, **48**, 357–364.
- 16 L. A. Paquette, R. D. Dura and I. Modolo, *Heterocycles*, 2007, **74**, 145.
- 17 H. Igeta, Y. Abe and A. Ohsawa, *Heterocycles*, 1982, **19**, 49.
- 18 V. Mamane and Y. Fort, *Tetrahedron Lett.*, 2006, **47**, 2337–2340.
- 19 Z. E. A. Chamas, O. Dietz, E. Aubert, Y. Fort and V. Mamane, *Org. Biomol. Chem.*, 2010, **8**, 4815–4818.
- 20 F. M. McMillan, H. McNab and D. Reed, *Tetrahedron Lett.*, 2007, **48**, 2401–2403.
- 21 V. Mamane, *Curr. Org. Chem.*, 2017, **21**, 1342–1392.
- 22 B. E. Maryanoff, H. C. Zhang, J. H. Cohen, I. J. Turchi and C. A. Maryanoff, *Chem. Rev.*, 2004, **104**, 1431–1628.
- 23 K. C. Sham, C. S. Lee, K. Y. Chan, S. M. Yiu, W. T. Wong and H. L. Kwong, *Polyhedron*, 2011, **30**, 1149–1156.
- 24 F. Kazemi, H. Sharghi and M. A. Nasser, *Synthesis*, 2004, 205–207.
- 25 V. Mamane, Z. Chamas, E. Aubert and Y. Fort, *RSC Adv.*, 2013, **3**, 19110–19116.